Registration-Based Patient-Specific Musculoskeletal Modeling Using High Fidelity Cadaveric Template Model

Yoshito Otake[1(✉)], Masaki Takao[2], Norio Fukuda[1], Shu Takagi[3], Naoto Yamamura[3], Nobuhiko Sugano[3], and Yoshinobu Sato[1]

[1] Graduate School of Information Science, Nara Institute of Science and Technology, Ikoma, Japan
otake@is.naist.jp
[2] Graduate School of Medicine, Osaka University, Osaka, Japan
[3] Department of Mechanical Engineering, The University of Tokyo, Tokyo, Japan

Abstract. We propose a method to construct patient-specific musculoskeletal model using a template obtained from a high fidelity cadaver images. Musculoskeletal simulation has been traditionally performed using a *string-type* muscle model that represent the line-of-forces of a muscle with strings, while recent studies found that a more detailed model that represents muscle's 3D shape and internal fiber arrangement would provide better simulation accuracy when sufficient computational resources are available. Thus, we aim at reconstructing patient-specific muscle fiber arrangement from clinically available modalities such as CT or (non-diffusion) MRI. Our approach follows a conventional biomedical modeling approach which first constructs a highly accurate generic *template* model which is then registered using the patient-specific measurement. Our template is created from a high-resolution cryosectioned volume and newly proposed registration method aligns the surface of bones and muscles as well as the local orientation inside the muscle (i.e., muscle fiber direction). The evaluation was performed using cryosectioned volumes of two cadavers, one of which accompanies images obtained from clinical CT and MRI. Quantitative evaluation demonstrated that the mean fiber distance error between the one estimated from CT and the ground truth was 4.16, 3.76, and 2.45 mm for the gluteus maximus, medius, and minimus muscles, respectively. The qualitative visual assessment on 20 clinical CT images suggested plausible fiber arrangements that would be able to be translated to biomechanical simulation.

Keywords: Muscle fiber modeling · Fiber arrangement · Clinical CT

1 Introduction

We aim at a patient-specific modeling of musculoskeletal structures for biomechanical simulation in pre-operative surgical planning and postoperative rehabilitation. While *string-type* muscle model simplifying each muscle as a few string

A. F. Frangi et al. (Eds.): MICCAI 2018, LNCS 11070, pp. 703–710, 2018.
https://doi.org/10.1007/978-3-030-00928-1_79

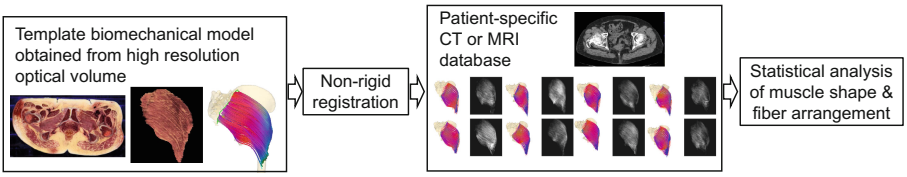

Fig. 1. Workflow of the proposed method. The shape and fiber arrangement of the target muscle (gluteus maximus in this figure) is obtained from a high-resolution optical volume of a cadaver specimen. The template is then registered to each subjects CT or MRI using the proposed non-rigid registration algorithm, from which the statistical model is created.

elements has been most commonly used in biomechanical simulations (such as in [12], etc.) by virtue of low computational cost and ease of modeling, 3D volumetric muscle models containing the muscle fiber architecture [3,14] have been investigated to improve accuracy of musculoskeletal simulation when sufficient computational resource is available. The modeling of muscle fiber arrangement has been attempted using medical imaging modalities such as ultrasound [15], diffusion tensor MRI [8], and micro CT [7], the limited field-of-view and long scan time precludes its use in clinical routine. On the other hand, the biomechanics community has proposed several method for modeling muscle fibers to achieve an accurate biomechanical simulation, one of which employs computational fluid dynamics [6] to obtain a physically plausible non-intersecting streamlines that connect origin and insertion areas. But the downside is its fidelity to patient-specific fiber arrangement.

Otake et al. [10] proposed a compromise solution in which a simple 3D geometric pattern representing fiber arrangement (e.g., a cluster of lines in a unit cube connecting top and bottom face) is spatially mapped to the muscle considering local orientation inside the muscle derived from the texture of patient's CT. Although it successfully modeled patient-specific and physically plausible fiber arrangement with a high-resolution optical volume, its robustness was limited especially for muscles with complicated fiber arrangement such as the gluteus medius in CT, and the authors demonstrated improved accuracy by addition of manually traced fiber lines, which should be highly operator dependent. Automated segmentation of musculoskeletal structures has been widely studied [1,11]. Especially, since the emergence of deep neural networks, it is approaching a viable option in clinical routine. Therefore, in this study, we assumed the segmentation label of the target bones and muscles are sou available. We propose a method to model patient-specific muscle fiber arrangement robustly from patient's medical images such as CT or (non-diffusion) MRI. Our approach follows a conventional biomedical modeling approach which first constructs a highly accurate generic *template* model, and then the template is non-rigidly registered to a noisy patient-specific image. Our template is created from a high-resolution cryosectioned volume [5] using the previously proposed method [10]. The contribution of this paper is twofold: (1) Introduction of a new cost function containing two

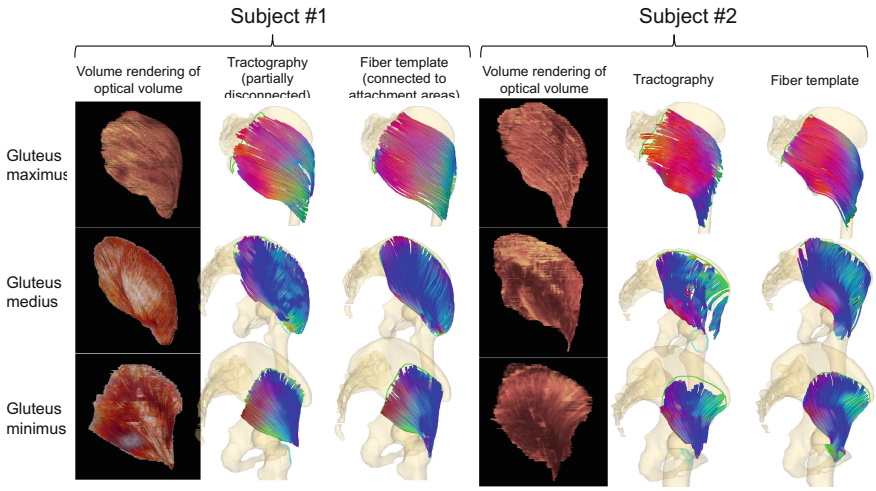

Fig. 2. High fidelity fiber arrangement templates obtained from optical image volume of two cadaver specimens in Visible Korean Human data set that were used as the ground truth in this study. A previously proposed algorithm [10] that fits a fiber template to the structure tensor field is employed. Tractography is also computed from the structure tensor field for comparison. The fitted fiber template correctly provided fiber lines that connect the origin and insertion areas, while tractography is partially disconnected due to noise in the tensor field. The color in the fiber rendering corresponds to the orientation at each line segment. X, Y, and Z components of the orientation vector were assigned to R, G, and B components.

data fitting terms, the surface fitness term and local orientation fitness term, and (2) evaluation with high-resolution optically acquired cryosection image volumes of two cadaver specimens. Quantitative evaluation of fiber arrangement is challenging also in brain tractography since obtaining the ground truth is difficult. We accomplished a validation with a highly reliable ground truth by using two series of cryosection images one of them accompanies CT and MR images.

2 Method

2.1 Overview of the Proposed Method

As illustrated in Fig. 1, the proposed method first construct a high fidelity template biomechanical model from a high resolution cryosection volume, then it is adapted to each patient using the information from patient-specific images. Since a large-scale image database is available for routinely used modalities such as CT and MR, the method allows statistical analysis of population-specific biomechanical parameters.

2.2 Construction of High Fidelity Fiber Arrangement Template and Preprocessing of Patient-Specific Images

Figure 2 shows the high fidelity fiber arrangement templates that we created from two optical cryosection image volumes (0.1 mm^3/voxel) using the method previously reported in [10]. As for the patient-specific image, CT or MRI, first, the regions of target bone and muscles are segmented. Although we used labels manually traced in 20 clinical CTs in this study, we confirmed with a larger scale CT database that automation of the segmentation using these 20 training data sets is viable with a deep neural network approach. The muscle attachment area was obtained using the method proposed by Fukuda et al. in [4]. Then, similar to [10], we obtain the local orientation within a neighborhood at each voxel by computing the eigenvector corresponding to the smallest eigenvalue of the gradient-based structure tensor [2]. A Gaussian filter (with standard deviation of σ_1) was applied to the image before computing gradient to suppress noise and after computing the gradient (with std. of σ_2) to smooth the tensor field. $\sigma_1 = 0.5$ mm and $\sigma_2 = 2$ mm were experimentally found to be effective in this method and used in the experiment below.

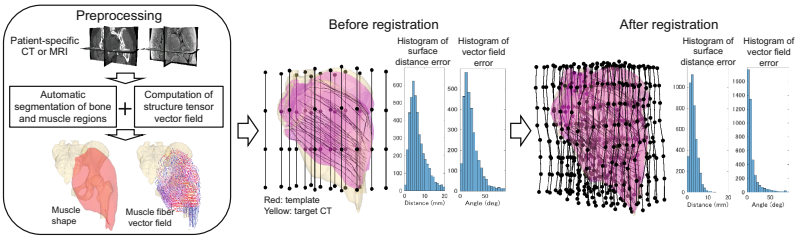

Fig. 3. The proposed non-rigid registration method with a cost function consisting of surface distance error and structure tensor vector field error.

2.3 Non-rigid Registration Using Shape and Local Orientation Cost

The proposed non-rigid registration and a representative registration result were illustrated in Fig. 3. The cost function consists of three terms, namely surface distance term (C_1), vector field difference term (C_2), and smoothness penalty term (g).

$$\hat{\mathbf{\Theta}} = \arg\min_{\mathbf{\Theta}} (1-\alpha) C_1(\mathbf{\Theta}) + \alpha C_2(\mathbf{\Theta}) + \lambda g(\mathbf{\Theta}) \tag{1}$$

The parameter α changes the balance between the two data fitness terms and λ is the regularization weight. Each term is as follows.

$$C_1(\mathbf{\Theta}) = \frac{1}{N_m} \sum_{i \in S_m} \min_{j \in S_f} ||p_{m,i}(\mathbf{\Theta}) - p_{f,j}|| + \frac{1}{N_f} \sum\nolimits_{j \in S_f} \min_{i \in S_m} ||p_{m,i}(\mathbf{\Theta}) - p_{f,j}||$$

where S_m, N_m and S_f, S_m represents the surface and the number of vertices of moving and fixed surfaces, respectively. In this study, the moving and fixed surfaces contain three objects, the pelvis, femur, and the target muscle. $p_{m,i}$ and $p_{f,i}$ represents ith vertex in S_m and S_f, respectively. This term represents the symmetric surface distance.

$$C_2(\mathbf{\Theta}) = -Dice(\Omega_f, \Omega_m)\frac{1}{N}\sum\nolimits_{i,j,k\in\Omega_f\cap\Omega_m} G(\theta_{i,j,k}(\mathbf{\Theta})); \sigma_{cost})$$

where Ω_f and Ω_m represent the regions covered by the moving and fixed surface, and $\theta_{i,j,k}$ represents the angular difference between vectors in the two vector fields at the voxed indexed by (i, j, k). $G(A; \sigma)$ is a Gaussian function with a standard deviation of σ. $g(\mathbf{\Theta})$ is a commonly used smoothness penalty term [13] represented as follows.

$$g(\mathbf{\Theta}) = \sum\nolimits_{\mathbf{i=1}}^{\mathbf{x}} \sum\nolimits_{\mathbf{j=1}}^{\mathbf{y}} \sum\nolimits_{\mathbf{k=1}}^{\mathbf{z}}$$
$$\left[\left(\frac{\partial^2 T}{\partial x^2}\right)^2 + \left(\frac{\partial^2 T}{\partial y^2}\right)^2 + \left(\frac{\partial^2 T}{\partial z^2}\right)^2 + 2\left(\frac{\partial^2 T}{\partial xy}\right)^2 + 2\left(\frac{\partial^2 T}{\partial yz}\right)^2 + 2\left(\frac{\partial^2 T}{\partial xz}\right)^2\right]$$

2.4 Evaluation Method

The cadaveric data set that we used in this study [5] includes optical image volumes of two specimens, and one of the specimen (denoted as *subject*1 in the figures) accompanies images obtained by clinical CT and MRI (voxel size: 1.0 mm^3). Thus, as shown in Fig. 4, we constructed a high fidelity template from the optical image of *subject*2 and registered to CT and MRI of *subject*1 and evaluated the result using a ground truth obtained from the optical image of *subject*1. As for the error metric, we employed the fiber distance error which is defined as the mean distance between pairs of corresponding points on the nearest fiber [9], which is one of the metrics used in evaluation of white matter fibers in brain tractography.

3 Results

Figures 5 and 6 show the results of fiber arrangement of the gluteus maximus, medius, and minimus muscles computed from CT and MRI using the proposed non-rigid registration. Figure 5 shows quantitative evaluation in *subject*1 where the accurate ground truth obtained from the optical image was available. The proposed method was compared also with two previous methods that 1) used the grid fitting to the CT [10] (denoted as *Previous method 2* in the figure) and 2) used computational fluid dynamics [6] that computes fiber arrangement from its surface shape (denoted as *Previous method 2* in the figure). Fiber distance error for the gluteus medius muscle (Fig. 5a) for the estimation from CT, MRI, previous method 1, and 2, were 3.76 ± 1.24 mm, 3.26 ± 0.85 mm, 4.15 ± 2.29 mm, 8.72 ± 4.40 mm, respectively. The *previous method 1* had larger number

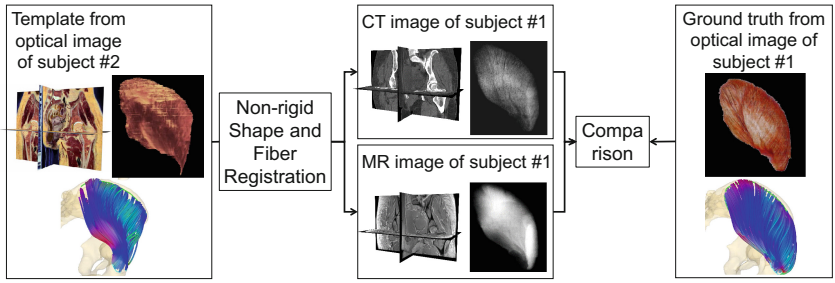

Fig. 4. Illustration of the evaluation scheme used in this study. Two cadaveric specimens are used. A high fidelity muscle fiber template obtained from an optical volume of one subject (subject 2) was registered to CT and MR images of the other subject (subject 1). The registration accuracy was evaluated by fiber distance error metric using the ground truth obtained from the optical volume of subject 1.

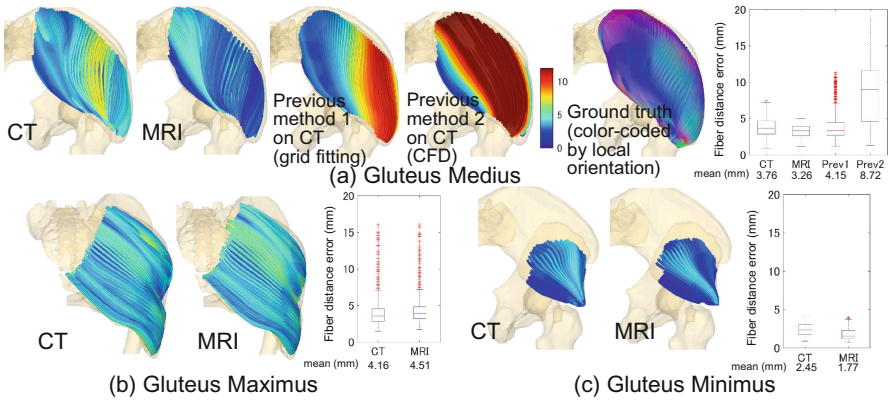

Fig. 5. Results of quantitative evaluation using the ground truth obtained from high resolution optical volume. The fiber arrangements estimated from CT and MRI in gluteus (a) medius, (b) maximus, and (c) minimus muscles were illustrated by the colormap corresponding to the fiber distance error from the ground truth.

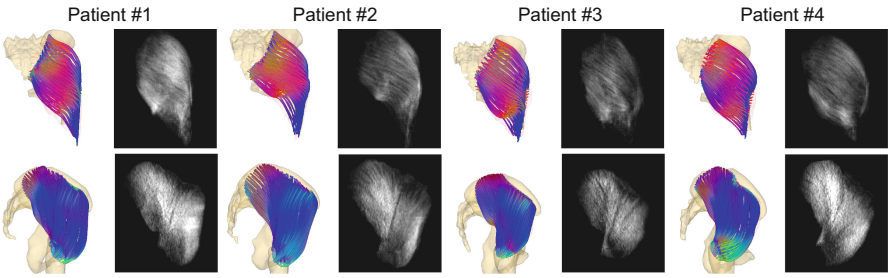

Fig. 6. Results of muscle fiber arrangement modeling of the gluteus maximus, and medius muscles of four representative patients (out of 20 patients analyzed in the study). The color corresponds to the local orientation (see the caption of Fig. 2)

of outliers in the anterior region (right side in the figure). We found that in this region of this subject, the amount of fat tissue was relatively low and there was almost no texture, resulting in a highly noisy structure tensor vectors. The proposed method was robust in this region owing to the cost function containing the fitness of the bone surface, where the attachment areas lay on, in addition to the vector field fitness. The *previous method 2* showed larger error overall, suggesting that the information from internal texture contributed significantly. The fiber distance errors for CT and MRI were 4.16 ± 2.34 mm, and 4.51 ± 2.38 mm, for the gluteus maximus and 2.45 ± 0.76 mm, and 1.77 ± 0.70 mm, for the gluteus minimus, respectively. Since the fiber distance error computes the average distance with the nearest fiber, the shorter fibers tend to show smaller error. Since fiber length is different between the muscles, direct comparison is difficult, but estimation from MRI shows smaller error in the gluteus medius, and minimus, and almost the same for the gluteus maximus. The results in Fig. 6 was obtained from clinical CTs, where no ground truth is available. Qualitative visual evaluation on the clinical CTs shown in Fig. 6 suggested a reasonable reconstruction for the three muscles.

4 Discussion and Conclusion

We proposed a non-rigid registration method with a cost function containing both surface distance error and the vector field angle error, and quantitatively evaluated its accuracy and demonstrated applications in patient-specific biomechanical modeling using a database of 20 clinical CTs. Compared to the previously proposed grid fitting method [10] that takes account for only the vector field, the proposed method was found to be more robust in the area with higher noise in the structure tensor field. Using the robust registration method, we proposed an approach to patient-specific biomechanical modeling using the high fidelity generic template model constructed from cadaveric images. One of the limitations in current study is that the evaluation used only two specimens only one of which has clinical CT and MRI. Enlarging the template database as well as introducing a new method to obtain the ground truth from clinical CTs are our ongoing work. Another potential future work is the statistical analysis using a large-scale CT database. The robustness of the proposed registration method even in the presence of noise in clinical CT would become a strong advantage in the large-scale cohort analysis of biomechanical parameters, since CT is the most common modality especially in the orthopedic surgery where the biomechanical simulation is most profitable.

Acknowledgment. This research was supported by MEXT/JSPS KAKENHI 26108004, JST PRESTO 20407, AMED/ETH the strategic Japanese-Swiss cooperative research program. The authors extend their appreciation to Professor Min Suk Chung (Ajou University School of Medicine) for providing us the Visible Korean Human dataset.

References

1. Andrews, S., Hamarneh, G.: The generalized log-ratio transformation: learning shape and adjacency priors for simultaneous thigh muscle segmentation. IEEE Trans. Med. Imaging **34**(9), 1773–1787 (2015)
2. Bigun, J.: Optimal orientation detection of linear symmetry. In: Proceedings of the IEEE First International Conference on Computer Vision, pp. 433–438 (1987)
3. Blemker, S.S., Delp, S.L.: Three-dimensional representation of complex muscle architectures and geometries. Ann. Biomed. Eng. **33**(5), 661–73 (2005)
4. Fukuda, N.: Estimation of attachment regions of hip muscles in CT image using muscle attachment probabilistic atlas constructed from measurements in eight cadavers. Int. J. Comput. Assist. Radiol. Surg. **12**(5), 733–742 (2017)
5. Jin, S.: Visible korean human: Improved serially sectioned images of the entire body. IEEE Trans. Med. Imaging **24**(3), 352–360 (2005)
6. Joshua, I., et al.: Fiber tractography for finite-element modeling of transversely isotropic biological tissues of arbitrary shape using computational fluid dynamics. In: Proceedings of the Conference on Summer Computer Simulation, pp. 1–6 (2015)
7. Kupczik, K.: Reconstruction of muscle fascicle architecture from iodine-enhanced microct images: a combined texture mapping and streamline approach. J. Theor. Biol. **382**, 34–43 (2015)
8. Levin, D.I.W.: Extracting skeletal muscle fiber fields from noisy diffusion tensor data. Med. Image Anal. **15**(3), 340–353 (2011)
9. O'Donnell, L.J., Westin, C.-F.: Automatic tractography segmentation using a high-dimensional white matter atlas. IEEE Trans. Med. Imaging **26**(11), 1562–1575 (2007)
10. Otake, Y., et al.: Patient-specific skeletal muscle fiber modeling from structure tensor field of clinical CT images. In: Descoteaux, M., et al. (eds.) MICCAI 2017, Part I. LNCS, vol. 10433, pp. 656–663. Springer, Cham (2017). https://doi.org/10.1007/978-3-319-66182-7_75
11. Popuri, K., Cobzas, D., Esfandiari, N., Baracos, V., Jägersand, M.: Body composition assessment in axial CT images using fem-based automatic segmentation of skeletal muscle. IEEE Trans. Med. Imaging **35**(2), 512–520 (2016)
12. Rajagopal, A., et al.: Full-body musculoskeletal model for muscle-driven simulation of human gait. IEEE Trans. Biomed. Eng. **63**(10), 2068–2079 (2016)
13. Rueckert, D., Sonoda, L.I., Hayes, C., Hill, D.L., Leach, M.O., Hawkes, D.J.: Non-rigid registration using free-form deformations: application to breast mr images. IEEE Trans. Med. Imaging **18**(8), 712–21 (1999)
14. Webb, J.D.: 3D finite element models of shoulder muscles for computing lines of actions and moment arms. Comput. Methods Biomech. Biomed. Eng. **17**(8), 829–37 (2014)
15. Zhou, Y.: Estimation of muscle fiber orientation in ultrasound images using revoting hough transform (RVHT). Ultrasound Med. Biol. **34**(9), 1474–81 (2008)